

Supplementary Information

Tunable Ni₂P@Polypyrrole nanocomposites for efficient hydrogen evolution and high-performance supercapacitor

Jong Hun Kim ^{†a}, Nguyen Duong Nguyen ^{†a,c}, Jaekyum Kim ^a, Won Tae Hong ^a, Kyoungsook Jin ^c,
Chengkai Xia ^d, Sangyul Baik ^{*e}, Jun Young Kim ^{*f}, Jun Young Lee ^a, Jung Kyu Kim ^{*a,b}

^a School of Chemical Engineering, Sungkyunkwan University (SKKU), 2066 Seobu-ro, Suwon, 16419, Republic of Korea

^b SKKU Advanced Institute of Nanotechnology (SAINT), Sungkyunkwan University (SKKU), 2066 Seobu-ro, Suwon 16419, Republic of Korea

^c Department of Chemistry, Korea University, 145 Anam-ro, Seoul, 02841, Republic of Korea

^d School of Materials Science and Engineering, North University of China, Taiyuan, 030051, Shanxi, China

^e Department of Mechanical Engineering, Sungkyunkwan University (SKKU), 2066 Seobu-ro, Suwon, 16419, Republic of Korea

^f Department of Biomedical-Chemical Engineering and Department of Artificial Intelligence, The Catholic University of Korea, Bucheon 14662, Republic of Korea

[†] These authors equally contributed to this work.

*Corresponding E-mails: bsy7863@skku.edu (S. Baik), june0112@catholic.ac.kr (J.Y. Kim), legkim@skku.edu (J.K. Kim)

Experimental section

Materials

Nickel (II) acetylacetonate ($\text{Ni}(\text{acac})_2$), 1-Octadecene (1-ODE), Oleylamine (OAm), Poly(vinylidene fluoride) (PVDF), N-Methyl-2-pyrrolidone (NMP) and commercial activated carbon were obtained from *Sigma Aldrich*. Pyrrole (Py) monomer was purchased from Daejung Chemicals. Tri-n-octylphosphine (TOP), and ammonium persulfate (APS) were purchased from Acros Organics. Nafion (5 wt%) and super P carbon black (SPCB) were purchased from Alfa Aesar. Nickel foam was purchased from iTASCO. Deionized water, chloroform, hexane, ethanol, and hydrochloric acid (HCl) were purchased from SamChum Chemical. GR grade chemicals were used as received without further purification. Polytetrafluoroethylene (PTFE, hydrophilic, 0.2 μm) was obtained from HYUNDAI MICRO.

Synthesis of nickel phosphide (Ni_2P) nanospheres

The Ni_2P nanospheres were synthesized following a slightly modified protocol from our previous study¹. First, $\text{Ni}(\text{acac})_2$ (250 mg, 0.97 mmol), OAm (25.6 mL, 78 mmol) and 1-ODE (18 mL, 56.4 mmol) were placed in a two-neck flask under nitrogen and magnetically stirred. The mixture was heated to 120°C at a heating rate of 10°C min⁻¹ under vacuum and maintained at this temperature for 1 h to effectively remove moisture and oxygen. After degassing, TOP (3 mL, 6.6 mmol) was directly injected into the solution, followed by heating the mixture to 320°C. The temperature was held constant at 320°C for 2.5 h, and then naturally cooled to the room temperature. The black precipitate was obtained from the solution by adding excess ethanol and separated through centrifugation (10,000 rpm, 10 min). Subsequently, black precipitate was further thoroughly washed at least three times using ethanol and hexane mixture (3:1 vol. ratio). Finally, Ni_2P nanospheres were dried under vacuum at 60°C for 24 h.

Synthesis of $\text{Ni}_2\text{P}@PPy$ nanocomposites

The $\text{Ni}_2\text{P}@PPy$ nanocomposite was synthesized *via* an *in-situ* oxidative polymerization method following a previously reported protocol². Initially, 50 mg of Py solution was prepared. Subsequently, Ni_2P nanospheres were dispersed in chloroform according to targeted composite compositions (200 mg for $\text{Ni}_2\text{P}@PPy$ -80%, 50 mg for $\text{Ni}_2\text{P}@PPy$ -50%, and 12.5 mg for $\text{Ni}_2\text{P}@PPy$ -20%) and sonicated for 1 h to achieve homogeneous dispersion. The Py solution was then combined with the dispersed Ni_2P suspension and subjected to additional sonication for 1 h. Next, the resulting mixture was cooled in an ice bath and stirred for 30 min. A pre-cooled solution of 0.025 M APS in 0.1 M HCl was slowly added dropwise to the reaction mixture while continuously stirring, maintaining a fixed molar ratio of APS to Py at 1:15. The polymerization reaction was carried out at approximately 5°C for 24 h with continuous stirring. The $\text{Ni}_2\text{P}@PPy$ was then collected by filtration using a PTFE membrane (0.2 μm pore size) and washed repeatedly with ethanol and deionized water. Finally, the nanocomposite was dried in a vacuum oven at 60°C overnight. As a control, pure PPy was synthesized following the identical procedure, omitting the addition of Ni_2P .

Synthesis of $\text{Ni}_2\text{P}@$ Activated carbon ($\text{Ni}_2\text{P}@AC$) nanocomposites

To compare the effect of support nature and interfacial interaction, $\text{Ni}_2\text{P}@AC$ nanocomposites were prepared by dispersing pre-synthesized Ni_2P and AC in ethanol,

followed by ultrasonication for 1 h to ensure a homogeneous dispersion. The resulting mixture was then collected, washed with deionized water, and dried in a vacuum oven at 60°C overnight. To ensure a controlled comparison, the amount of activated carbon (50 mg) was fixed to match the pyrrole monomer content used in the Ni₂P@PPy system, and the Ni₂P loading was adjusted accordingly to maintain consistent composition.

Material characterizations

The powder X-ray diffraction (XRD) patterns were acquired with Cu K α radiation on an X-ray diffractometer (Bruker D8 Advance, Germany). High resolution transmission electron microscope (HR-TEM) images were obtained using Cs-corrected TEM with an acceleration voltage of 200 kV (JEM ARM 200F, JEOL, Japan). X-ray photoelectron spectroscopy (XPS) measurements were carried out using ESCALAB 250 (Thermo Fisher Scientific, USA) with Al K α as the X-ray source. Fourier Transform Infrared Spectroscopy (FT-IR) spectra were collected on a IRTracer-100 (Shimadzu Scientific, Japan, NFEC-2024-12-302272), with samples prepared by KBr pelletizing. Raman spectra were acquired on a LabRam Aramis (Horiba Jobin Yvon, Japan) Raman spectrometer with a 532 nm excitation wavelength from an Ar ion laser source.

Electrochemical characterizations

All electrochemical measurements were performed with an electrochemical workstation (CHI 705E, CH Instruments) in a standard three-electrode system, with Hg/HgO as a reference electrode and Pt wire as a counter electrode. For hydrogen evolution reaction (HER), measurements were carried out in 1.0 M KOH electrolyte. Catalyst ink was prepared by dispersing 4 mg of catalyst and 30 μ L of Nafion (5 wt%) in 1 mL of water/isopropanol mixture (1:1 vol. ratio), followed by ultrasonication for 30 min. Subsequently, 7.5 μ L of the catalyst ink was dropped onto a nickel foam electrode, which was then dried overnight in a vacuum oven. For supercapacitor measurements, electrochemical tests were conducted in 3.0 M KOH electrolyte. The active material was mixed with SPCB and PVDF in NMP solvent at a weight ratio of 0.7:0.2:0.1. The prepared slurry was coated onto the nickel foam substrate and then dried in a vacuum oven for 24 h before the electrochemical measurements. The electrochemical impedance spectroscopy (EIS) was measured in the frequency range of 10⁻²-10⁵ Hz at the open-circuit potential. The *in-situ* Raman characterization was performed using a Raman electrochemical cell (Redoxme AB, Sweden) coupled to an electrochemical workstation (CHI 705E, CH Instruments). The Raman cell incorporated a standard three-electrode configuration, consisting of Ag/AgCl reference electrode and a Pt wire counter electrode, while a catalyst-coated carbon cloth served as the working electrode. Raman spectra were collected during chronoamperometric measurements in KOH alkaline electrolyte at several applied potentials, using an AIRSight Raman microscope (Shimadzu Scientific, Japan, NFEC-2024-12-302272) equipped with a 532 nm laser (55 mW) and a 50X objective lens.

Calculation of specific capacitance and capacitance contribution:

To calculate the specific capacitance, the following formula was used.

$$C = \frac{i\Delta t}{M\Delta V} \quad (1)$$

Where C , i , M , ΔV , and Δt indicate the specific capacitance (F g⁻¹), discharging current (mA), mass of active materials (mg), potential window (V), and total discharge time (sec),

respectively. To elucidate the energy storage contribution of the electrode, the following power-law formula was used³.

$$i = av^b \quad (2)$$

Where i is peak current (mA), v is the scan rate (mV s⁻¹), and the b value is acquired from the slope of the fitted linear plot of $\log(i)$ vs. $\log(v)$ at a certain potential. The relative contributions of capacitive-controlled (k_1v) and diffusion-controlled ($k_2v^{1/2}$) mechanisms were quantified using the Dunn method, based on the following equations:

$$i(V) = k_1v + k_2v^{1/2} \quad (3)$$

$$\frac{i(V)}{v^{1/2}} = k_1v^{1/2} + k_2 \quad (4)$$

Where k_1 and k_2 are constants obtained from equation (3), representing the slope (k_1) and intercept (k_2) respectively.

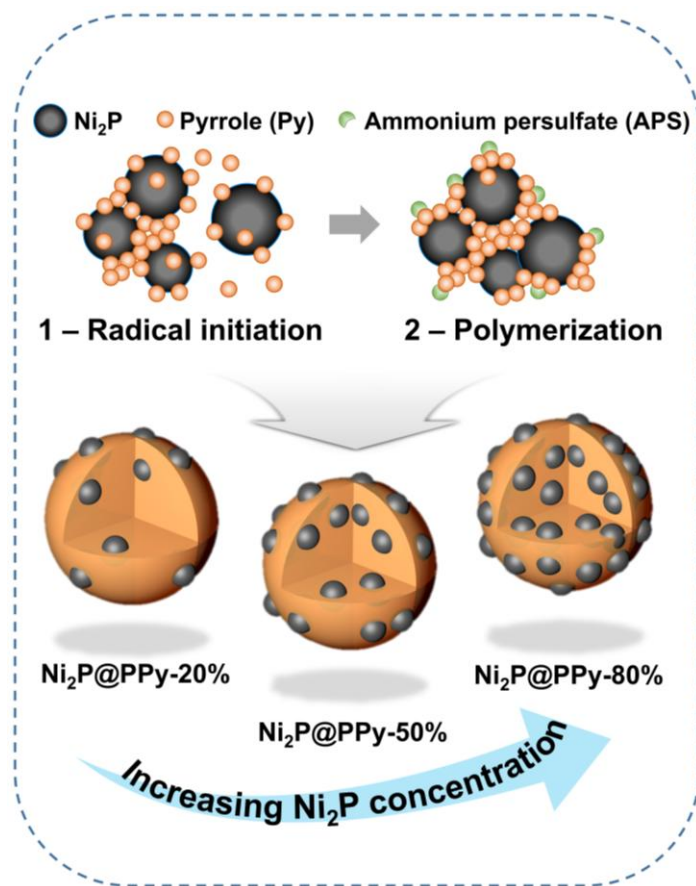


Fig. S1 Schematic illustration of Ni₂P@PPy nanocomposite

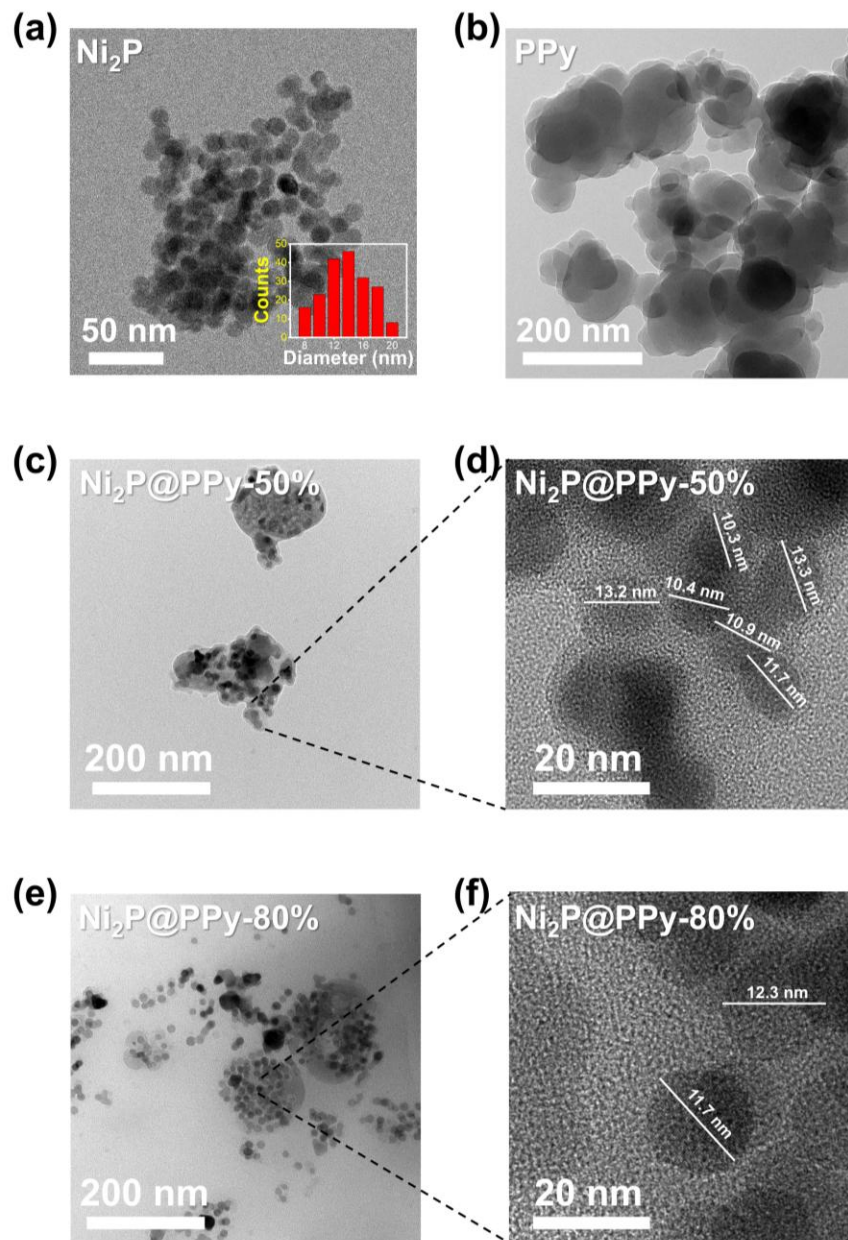


Fig. S2 HR-TEM images of (a) pristine Ni₂P, (b) pristine PPy, (c-d) Ni₂P@PPy-50%, (e-f) Ni₂P@PPy-80%.

The Ni₂P nanospheres in all Ni₂P@PPy nanocomposites retained the same average particle size as the pristine Ni₂P (14 ± 6 nm) as confirmed by the particle size distribution in Fig S2(a). This consistency indicates that the chemical oxidative polymerization process does not alter the structural integrity of Ni₂P.

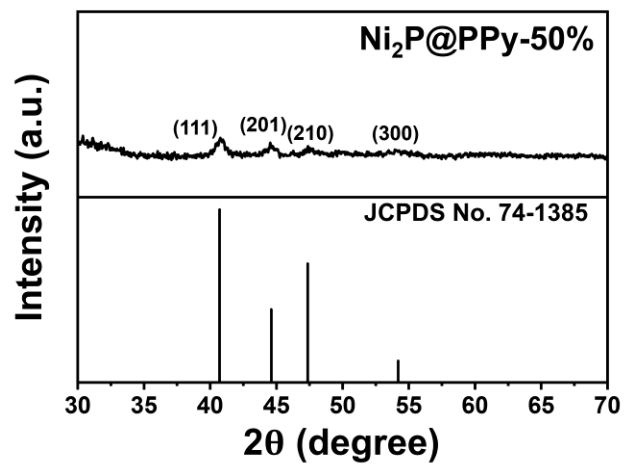


Fig. S3 XRD patterns of Ni₂P@PPy-50%

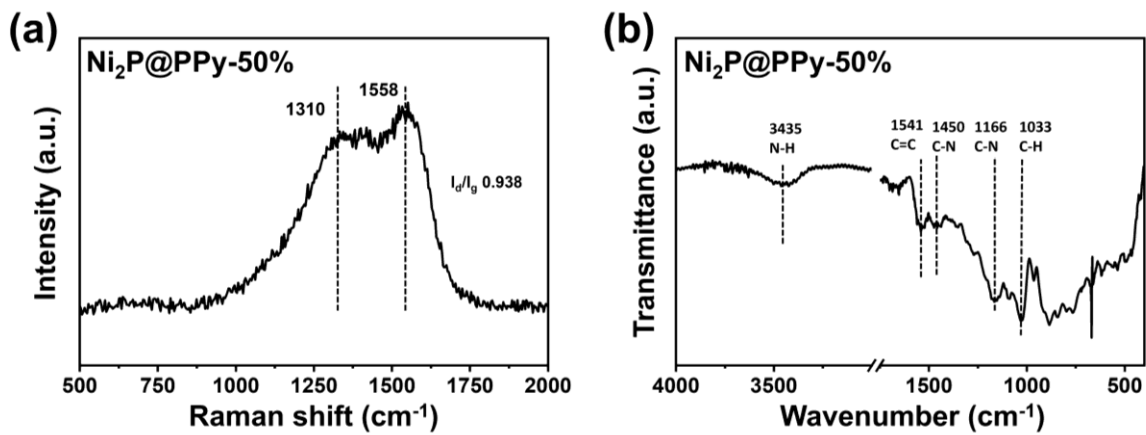


Fig. S4 (a) Raman spectra and (b) FT-IR spectra of Ni₂P@PPy-50%.

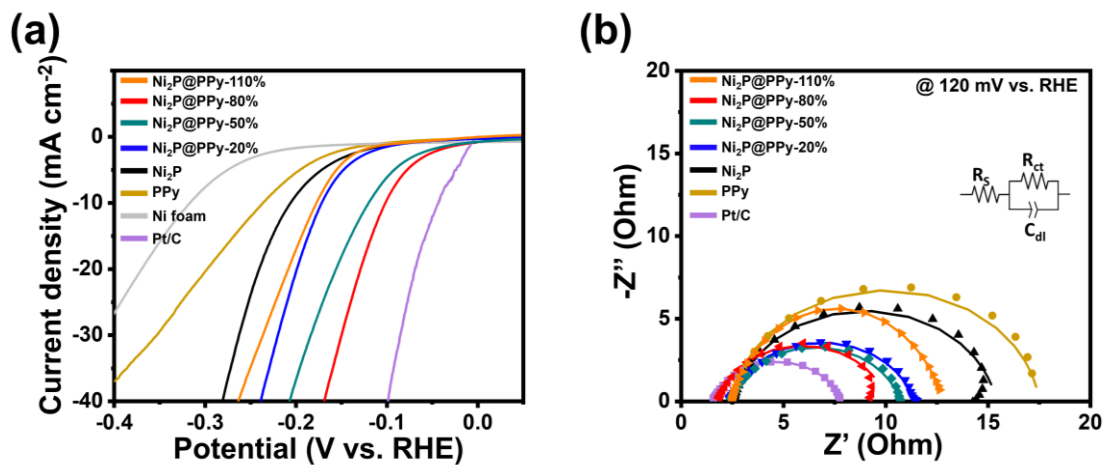


Fig. S5 HER performance of Ni₂P@PPy composites, pristine Ni₂P, pristine PPy, bare Ni foam, and Pt/C in 1.0 M KOH (a) the *iR*-compensated LSV polarization curves, (b) Nyquist plots as prepared electrodes.

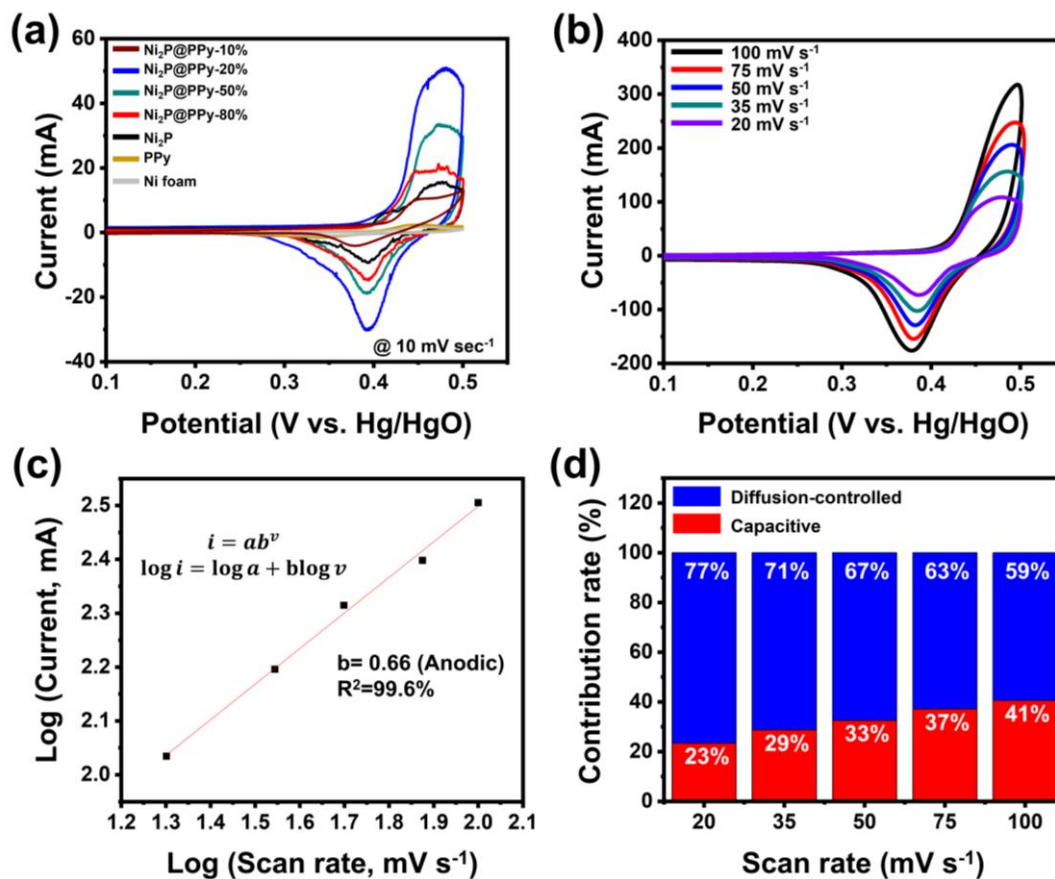


Fig. S6 (a) Cyclic voltammetry (CV) of Ni₂P@PPy-based electrodes, pristine Ni₂P, pristine PPy, and Ni foam in 3.0 M KOH, (b) CV responses for Ni₂P@PPy-20% at various scan rate (20-100 mV s⁻¹), (c) the b value fitted from anodic peaks of the Ni₂P@PPy-20%, (d) contribution rate of Ni₂P@PPy-20% at different scan rates.

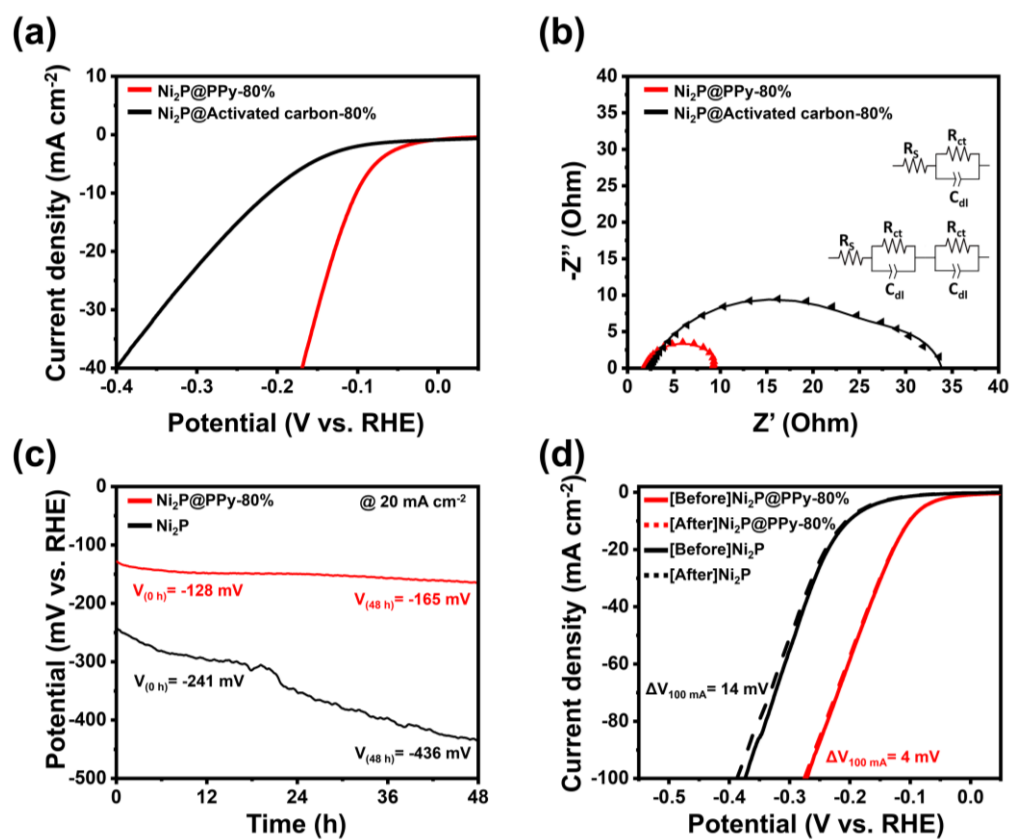


Fig. S7 (a) LSV curves and (b) Nyquist plots of Ni₂P@PPy-80% and Ni₂P@Activated carbon-80%, (c) time-dependent chronopotentiometry curves, and (d) long-term stability before and after 2,000 cycles for Ni₂P@PPy-80% and pristine Ni₂P electrodes.

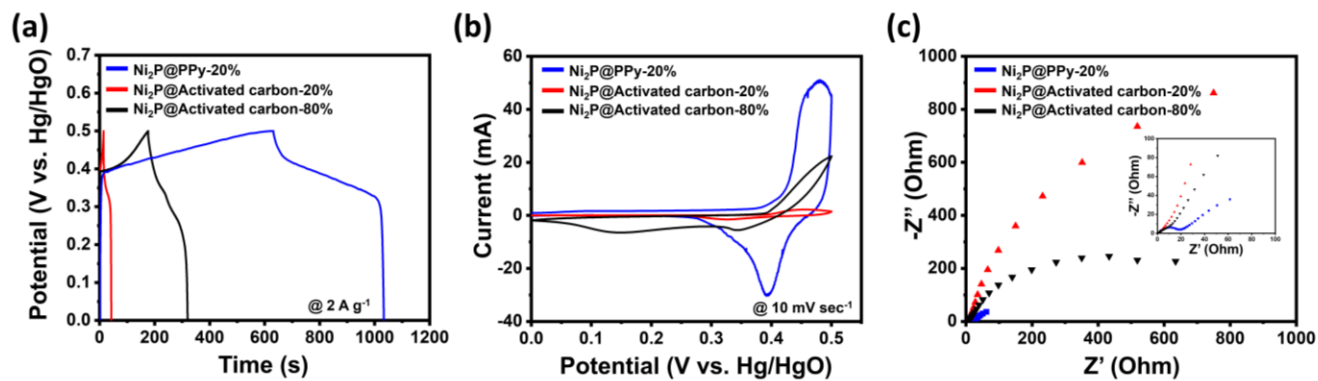


Fig. S8 (a) GCD curves, (b) CV curves and (c) Nyquist plots of Ni₂P@PPy-20%, Ni₂P@AC-20%, and Ni₂P@AC-80% electrodes.

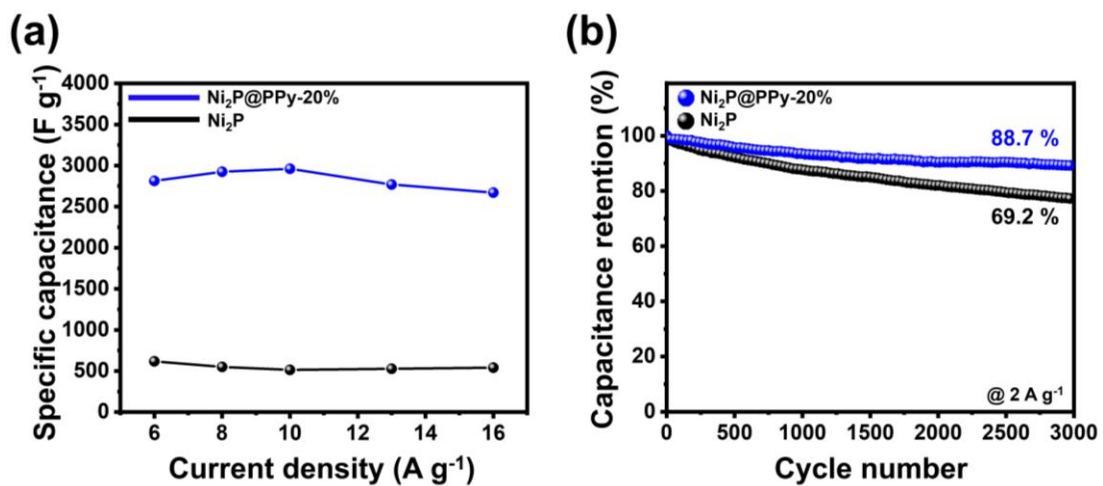


Fig. S9 (a) Variation of specific capacitance as a function of current, (b) specific capacitance retention at the 2 A g⁻¹.

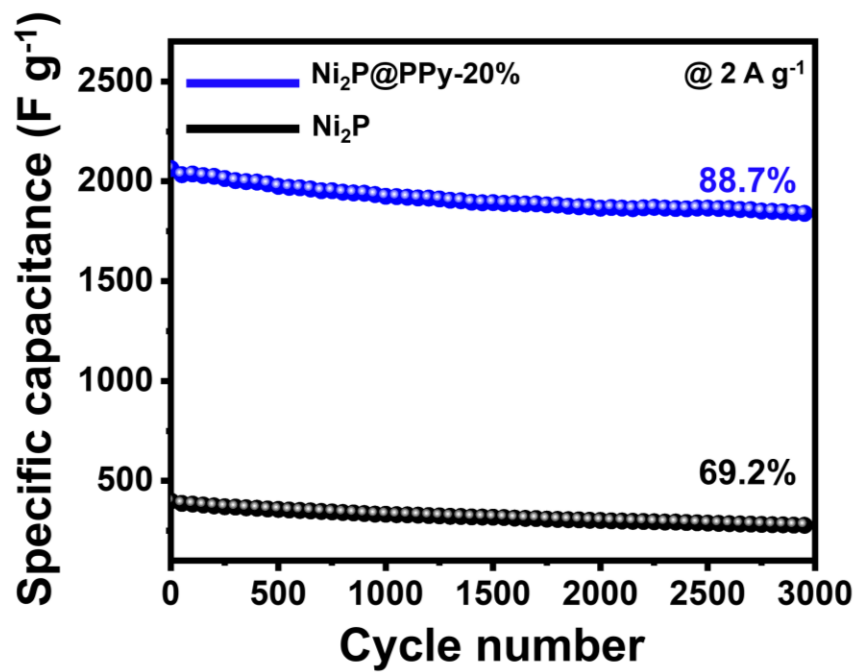


Fig. S10 3,000 cycles operational test for Ni₂P@PPy-20% and pristine Ni₂P electrodes.

Table S1. Ratio of positively charged N / total N peak area ratio for Ni₂P@PPy-20% and Ni₂P@PPy-80%.

Samples	Positively charged N/ total N
Ni ₂ P@PPy-20%	16.09%
Ni ₂ P@PPy-80%	38.55%

Table S2. Electrochemical impedance spectroscopic fitted circuit parameters for HER.

Samples	R_s (Ω)	R_{ct} (Ω)
Ni ₂ P@PPy-110%	2.4	10.2
Ni ₂ P@PPy-80%	1.8	7.8
Ni ₂ P@PPy-50%	2.4	8.3
Ni ₂ P@PPy-20%	2.5	9.0
Pristine Ni ₂ P	2.7	12.8
Pristine PPy	2.6	15.0
Pt/C	1.6	6.3

Table S3. Electrochemical impedance spectroscopic fitted circuit parameters for supercapacitor.

Samples	R_s (Ω)	R_{ct} (Ω)
Ni ₂ P@PPy-80%	1.6	61.7
Ni ₂ P@PPy-50%	1.3	32.2
Ni ₂ P@PPy-20%	1.4	17.2
Ni ₂ P@PPy-10%	1.2	79.4
Pristine Ni ₂ P	1.5	40.0
Pristine PPy	1.3	103.9

Table S4. Comparison of HER and Supercapacitor performance of Ni₂P@PPy and recently reported related materials.

Materials	Overpotential (mV) @10 mA cm ⁻²	Tafel slope (mV/dec)	Specific capacitance (F g ⁻¹)	3 electrode Capacity retention (%) / number of cycles	References
Ni ₂ P@PPy	102 mV	88	2046.7 (@2 A g ⁻¹)	88.7% / 3,000	This work
Ni ₂ P/NPMC-0.5	96 mV	75	-	-	<i>Applied Surface Science</i> 694 (2025): 162833.
Ni ₂ P/Ni(OH) ₂	99.8 mV	93.2	-	-	<i>ChemSusChem</i> 18.24 (2025): e202501589.
Ni ₂ P/SSM	120 mV	114.77	-	-	<i>Materials Letters</i> 351 (2023): 134998.
Sm-doped Ni ₂ P	130.6 mV	67.8	-	-	<i>Scientific Reports</i> 14.1 (2024): 16818.
Ni ₂ P-NiMoO _x /NF	91 mV	60.1	-	-	<i>ACS Catalysis</i> 13.14 (2023): 9792-9805.
N-doped Ni ₂ P	110 mV	108	-	-	<i>International Journal of Hydrogen Energy</i> 51 (2024): 713-724.
(Co,Ni)OOH-400	149 mV	41	-	-	<i>Nano Research</i> 16.5 (2023): 6552-6559.
Ni ₃ Fe@NC	116.2 mV	134.43	-	-	<i>Applied Surface Science</i> 614 (2023): 156189.
PPy/Ni ₂ P	-	-	476.5 (@1 A g ⁻¹)	89% / 3,000	<i>Journal of Solid State Electrochemistry</i> 23.12 (2019): 3409-3418.

PPy/Ni ₂ P/GO	-	-	741.5 (@1 A g ⁻¹)	89.76%/ 5,000	<i>Journal of Solid State Electrochemistry</i> 25.7 (2021): 1975-1985.
Ni ₂ P	-	-	1330 (@1 mV s ⁻¹)	-	<i>Journal of Physics: Energy</i> 7.4 (2025): 045022.
Ni ²⁺ -doped polypyrrole	-	-	506 (@1 mV cm ⁻²)	66%/1,000	<i>Ionics</i> 30.12 (2024): 8481- 8494.
Ni ₂ P/NCHTs	-	-	1086 (@ 1 A g ⁻¹)	-	<i>Journal of Energy Storage</i> 99 (2024): 113265.
Ni ₂ P ₂ O ₇ /NF@P Py	-	-	498 (@ 1 A g ⁻¹)	97.4%/10,000	<i>Inorganic Chemistry Communications</i> 151 (2023): 110634.
NiCoMn MOFs/PANI/rG O	-	-	1007 (@ 1 A g ⁻¹)	115%/1,500	<i>RSC advances</i> 14.3 (2024): 2102-2115.

While the HER and supercapacitor performance of Ni₂P@PPy are comparable to those of previously reported materials, the key advantage of our system lies in its ability to deliver both functionalities within a single material platform through simple composition control.

1. D. N. Nguyen, T. K. C. Phu, J. Kim, W. T. Hong, J.-S. Kim, S. H. Roh, H. S. Park, C.-H. Chung, W.-S. Choe, H. Shin, J. Y. Lee and J. K. Kim, *Small*, 2022, **18**, 2204797.
2. A. Malinauskas, *Polymer*, 2001, **42**, 3957-3972.
3. T. S. Mathis, N. Kurra, X. Wang, D. Pinto, P. Simon and Y. Gogotsi, *Advanced Energy Materials*, 2019, **9**, 1902007.